Basics of channeling ion implantation

Masahiko Aoki

When the ion is implanted along a specific crystal axis of a single crystal, there is the phenomenon in which incident ions penetrate deeply along the crystal axis, and this is called channeling ion implantation. Recently, there have been reports of ion implantation using the channeling phenomenon in the field of compound semiconductor devices (1). According to this report, the research and development including an ion implanter is progressing with the aim of applying it to power devices using silicon carbide. Therefore, to make it easier to understand the channeling phenomenon, we have taken up the basic theory such as energy loss due to the collision between the incident ion and the target atom. At the same time, we will also introduce the analysis results by MARLOWE to provide information to deepen understanding (2).

1. Interatomic potential
2. Nuclear Stopping power
3. Nonlocal electronic stopping power
4. Local electronic stopping power
5. Example of channeling implantation
6. Effect of target temperature

1. Interatomic potential

The interatomic potential between the incident ion and the target atom is defined in consideration of the effect that the Coulomb field by the nucleus is shielded by the core electrons (3).

$$V(r) = \frac{Z_1 Z_2 e^2}{4\pi\varepsilon_0 r} \Phi\left(\frac{r}{a}\right)$$

The shielding function (Φ) is defined as follows.

$$\Phi(x) = 0.1818e^{-3.2x} + 0.5099e^{-0.9423x} + 0.2802e^{-0.4029x} + 0.02817e^{-0.2016x}$$

$$a = \frac{0.8854a_0}{{Z_1}^{0.23} + {Z_2}^{0.23}}$$

a_0:Bohr radius

Figure 1 shows the difference in the interatomic potential distribution with and without the shielding function.

Fig. 1 ：Al-Si inter-atomic potential

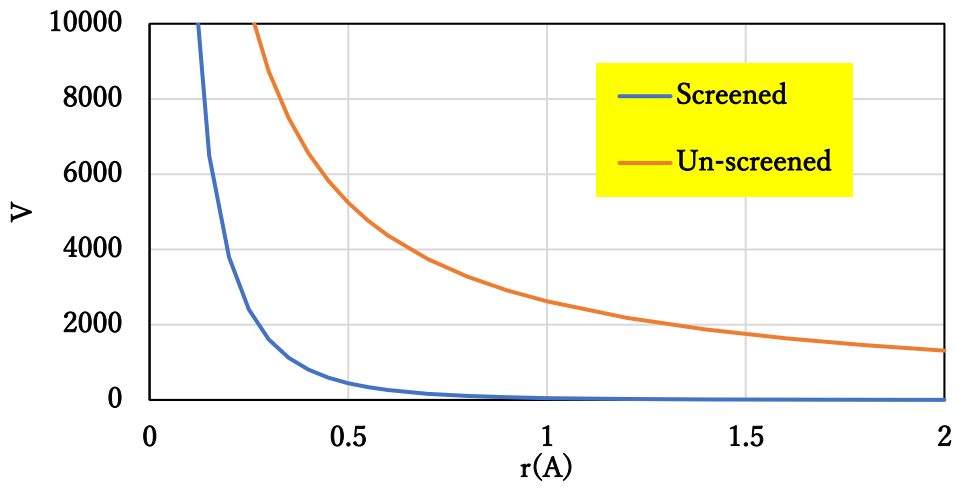

To consider the effect of the combination of the incident atom and the target atom, the shielding length is corrected by the coefficient γ as follows.

$$\frac{a}{\gamma}$$

When the correction coefficient (γ) is smaller than 1.0, the Coulomb field expands and the interaction region becomes larger, as shown in Fig. 2. As a result, it is estimated that the energy loss will increase. In other words, it becomes difficult for incident ions to penetrate deeply.

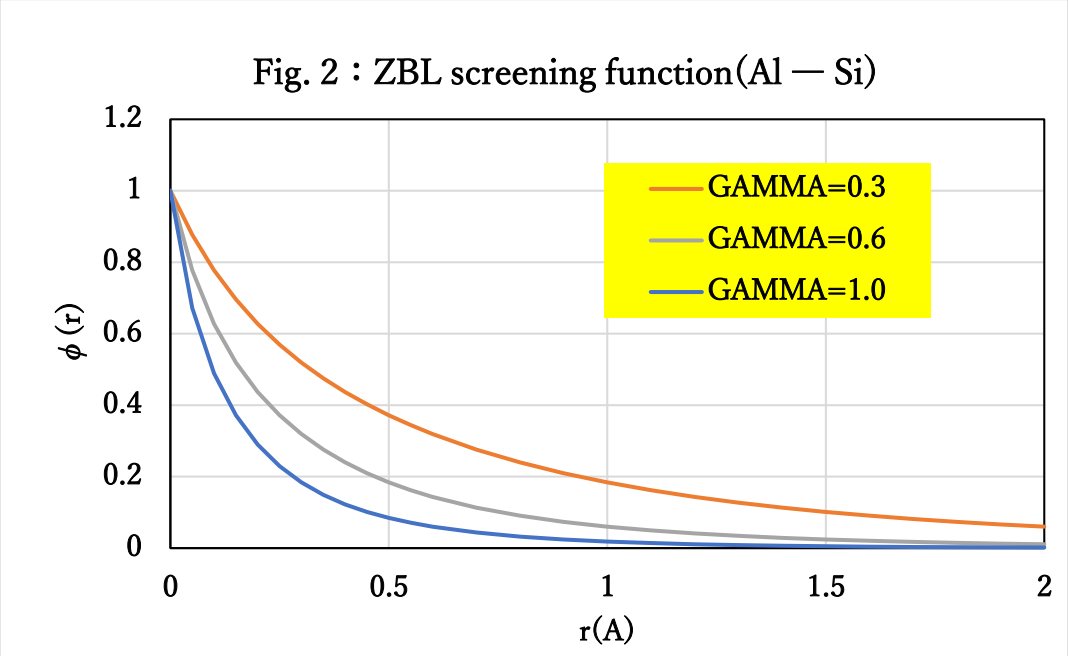

2. Nuclear Stopping power

The stopping power of collisions with nucleus has the energy dependence. Figure 3 shows the results of comparing the stopping power of Ziegler's analytical formula with that of SRIM. The results of Ziegler's analytical formula in a wide energy range show reasonable agreement with SRIM (4).

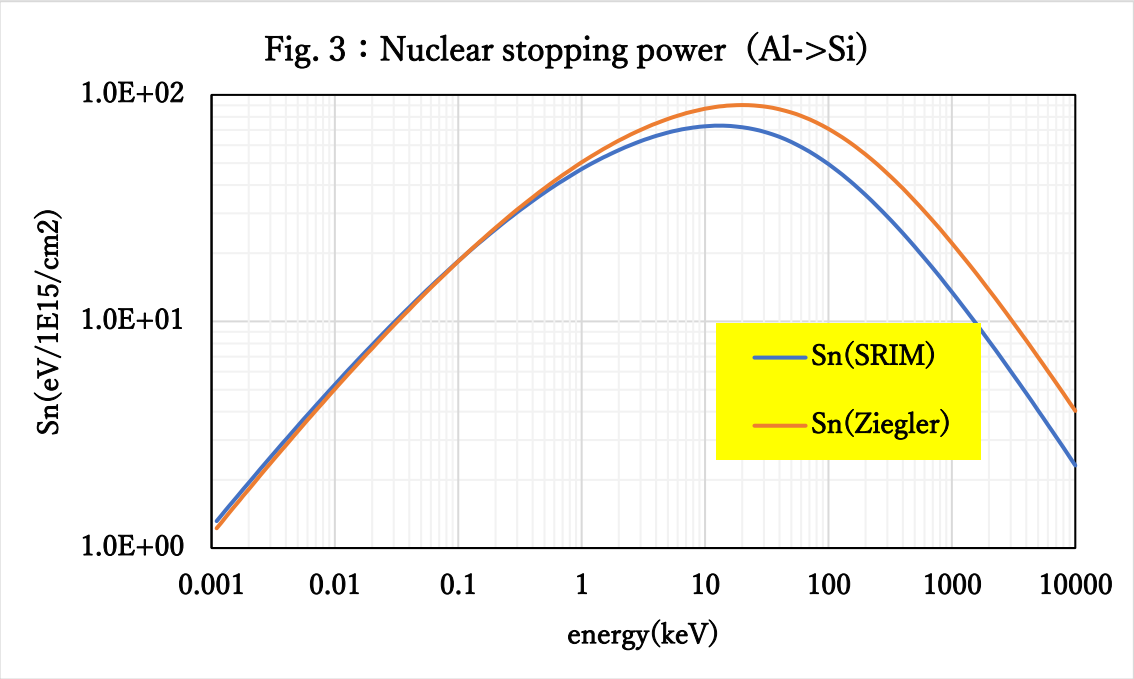

3. Nonlocal electronic stopping power

When an incident ion collides with a target atom, it is necessary to consider the nonlocal electronic stopping power and local electronic stopping power. The nonlocal electronic stopping power is expressed based on the LSS theory that the electronic energy loss of an incident ion is proportional to the square root of energy (5).

$$S_e = k \times \sqrt{E}$$

$$k = 8\pi h a_0 \sqrt{2} \frac{Z_1^{\frac{7}{6}} Z_2}{\left(Z_1^{\frac{2}{3}} + Z_2^{\frac{2}{3}}\right)^{\frac{3}{2}} \sqrt{M_1}}$$

Figure 4 shows the energy loss value (Se) due to electrons and the energy loss value (Sn) due to nucleus obtained by SRIM.

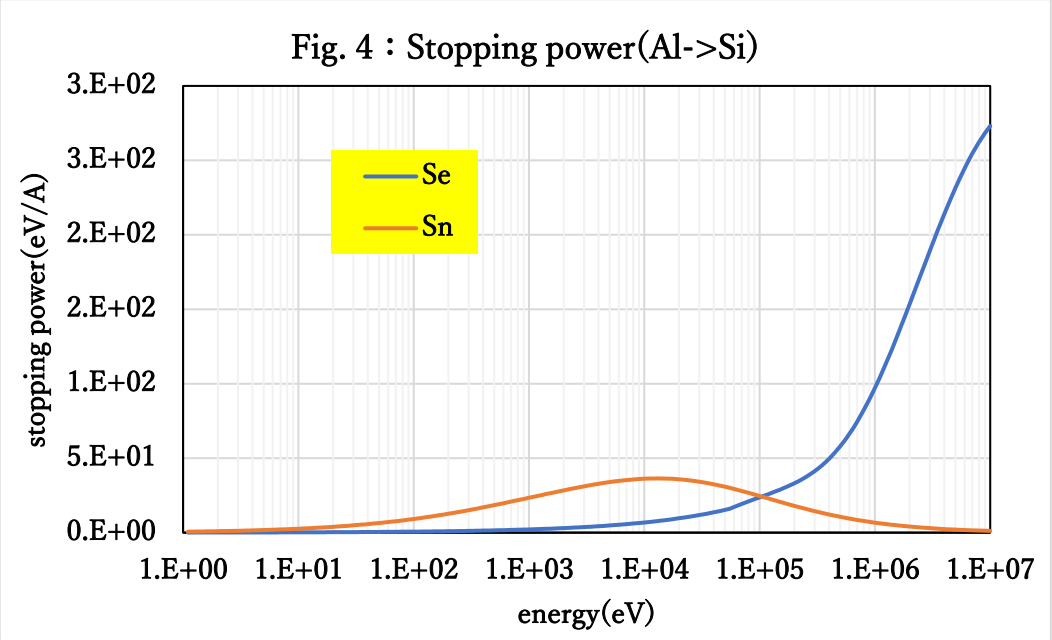

The stopping power by LSS theory is the classical approximation. When the velocity of the incident ion exceeds the Fermi velocity, the inner-shell electrons are stripped off, so it is necessary to adopt an energy loss model that considers the relativistic effect. For example, for boron into silicon, the LSS theory can be applied up to 2.2 MeV, and for arsenic, the 194 MeV is the applicable limit energy. Furthermore, from this graph, the nuclear stopping power (Sn) is dominant below 100 keV. The collision with the electron causes energy loss, and finally the scattered atoms will stop.

4. Local electronic stopping power

On the other hand, the following model in which the local electronic stopping power depends on the impact parameter (p) has been reported (6). The shield length (a) is corrected using the coefficient γ.

$$Q(p,E) = k\sqrt{E}\frac{1}{2\pi\left(\frac{a}{\gamma}\right)^2}exp\left(-\frac{r(p,E)}{\left(\frac{a}{\gamma}\right)}\right)$$

where k is the nonlocal stopping power value defined in the previous section. Furthermore, r (p, E) represents the interatomic distance.

The total stopping power is evaluated by integration as follows.

$$S_e(E) = 2\pi \int_0^{\infty} pQ(p,E)dp = k\sqrt{E}\sigma(\epsilon)$$

To explain the meaning of the impact parameter (p), Fig. 5 shows the two-body scattering collision phenomenon between the incident ion and the target atom. A small impact parameter (p) means that the ion is incident near the target atom. On the other hand, the large impact parameter means that the ion is incident at a place far from the target atom position. If the impact parameter is small, it will be more susceptible to scattering from the target atom, and if the impact parameter is large, it will be less susceptible to scattering from the target atom.

Fig. 5 two-body scattering

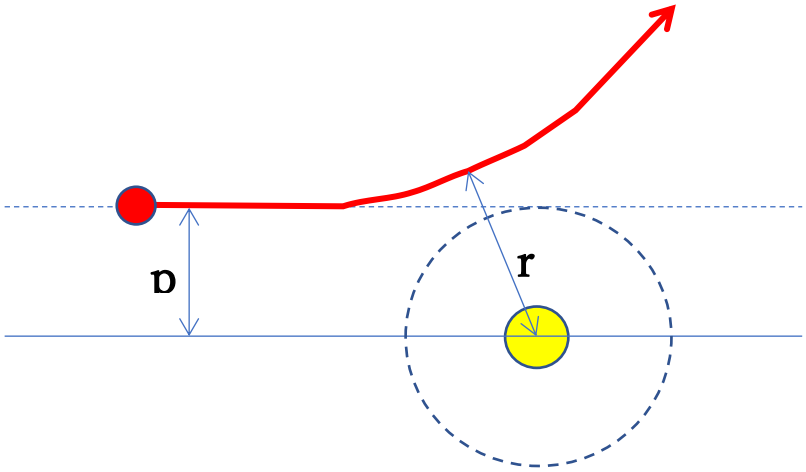

Figure 6 shows the dependence of the correction factor for local stopping power. In a certain collision coefficient (p_1), the energy loss increases as the value of the correction coefficient (γ) increases. It also reflects that the energy loss increases as the energy of the incident ions increases.

Fig. 6：Energy loss vs. gamma (impact parameter: $p=p_1$)

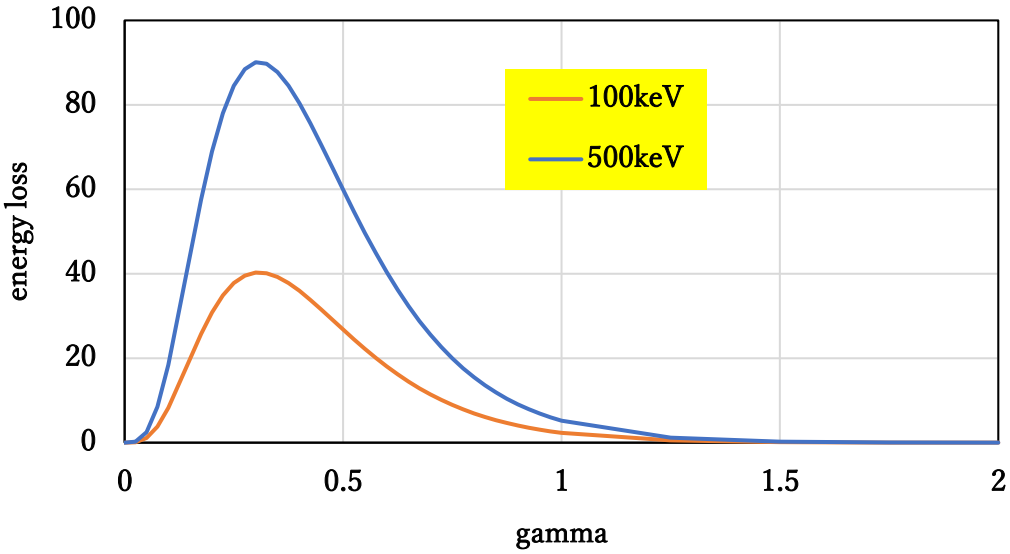

On the other hand, when the impact parameter (p_2) is larger than p_1, the distance to the target atom becomes long and the interaction becomes weak, so the energy loss becomes small as shown in Fig. 7.

Fig. 7：Energy loss vs. gamma (impact parameter: $p=p_2>p_1$)

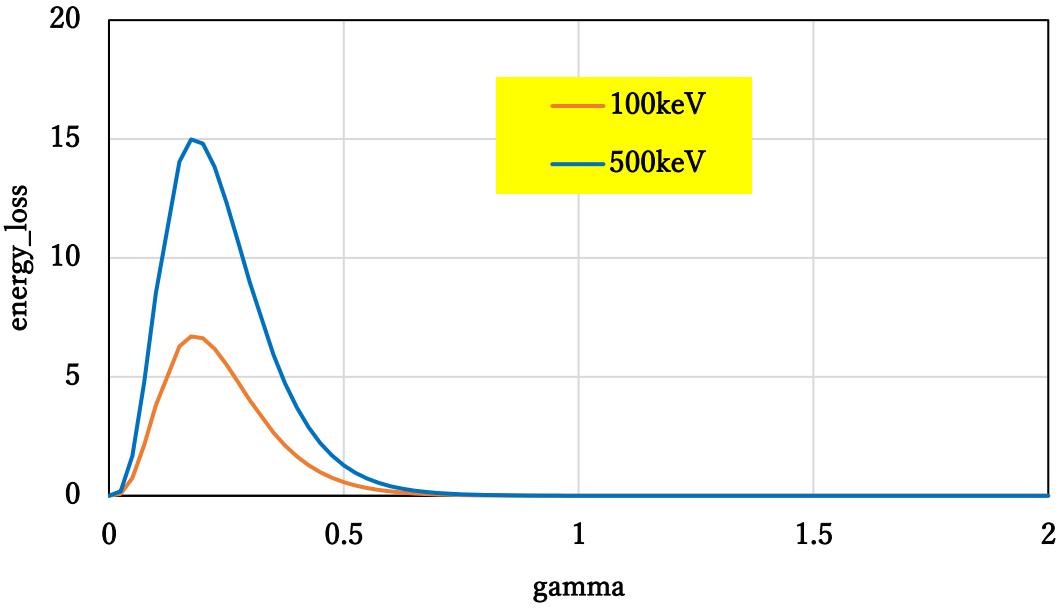

In this way, the difference of energy loss is depending on where the incident ion passes on the crystal axis, that is, the penetration depth of the ion differs. This is the essence of channeling implantation. Furthermore, from the graphs in Fig. 6 and Fig. 7, the value of γ has a large effect on energy loss. In other words, optimizing the value of γ is the key to correctly reproducing the channeling phenomenon.

5. Example of channeling implantation

The deviation of the ion incident direction from the crystal axis affects the channeling implantation. If the incident ion implanted on the target with a deviation of a certain angle or more, it will repeatedly collide with the atoms at the lattice position, losing energy and preventing it from penetrating deeply as shown in Fig. 8.

Fig. 8 ion channeling

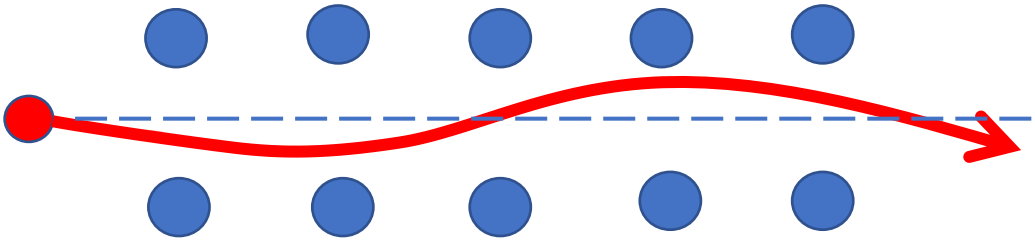

This critical channeling angle is expressed by the following equation (7).

$$\theta_{critical} \propto \sqrt{\frac{Z_1 Z_2 e^2}{E d_{row}}}$$

Here, the d_{row} represents the crystal lattice spacing in the ion incident direction. As shown in Fig. 9, the higher the incident energy (E), the smaller the critical angle, and a slight deviation from the crystal axis affects channeling.

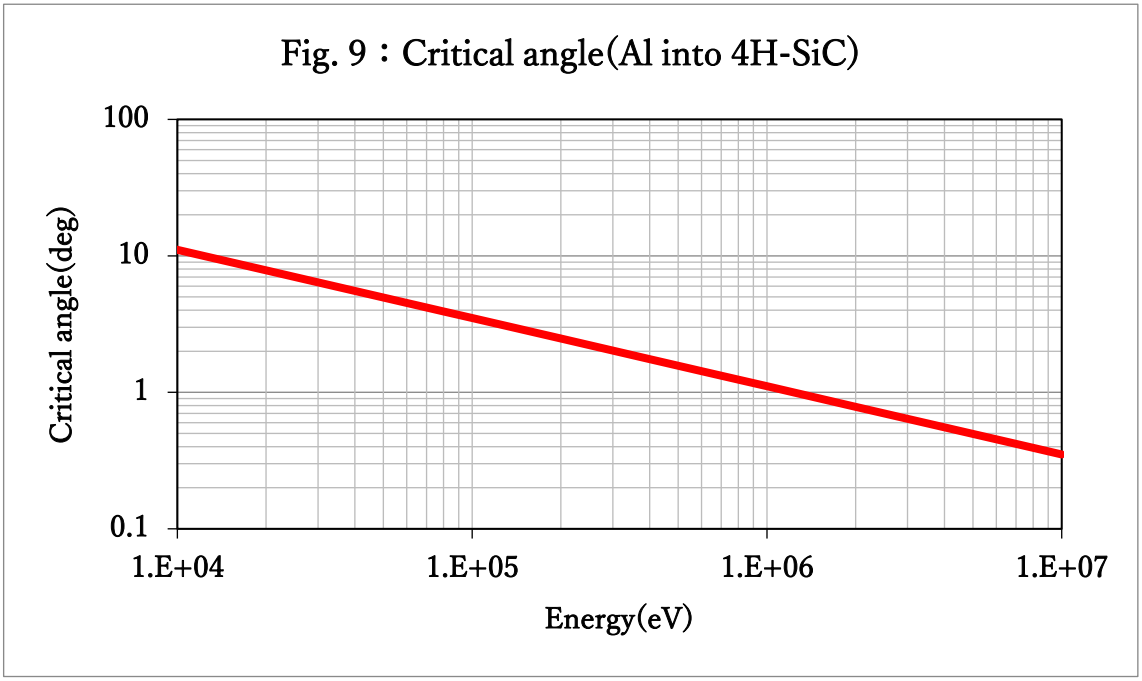

As an example of channeling implantation, the high energy channeling implantation will be introduced. Figure 10 shows the profile obtained by simulation when 8 MeV aluminum ions are implanted along the c-axis of 4H-SiC. The aluminum ions extend to about 8 microns. This simulation result was actually in good agreement with the SIMS result of channeling implantation.

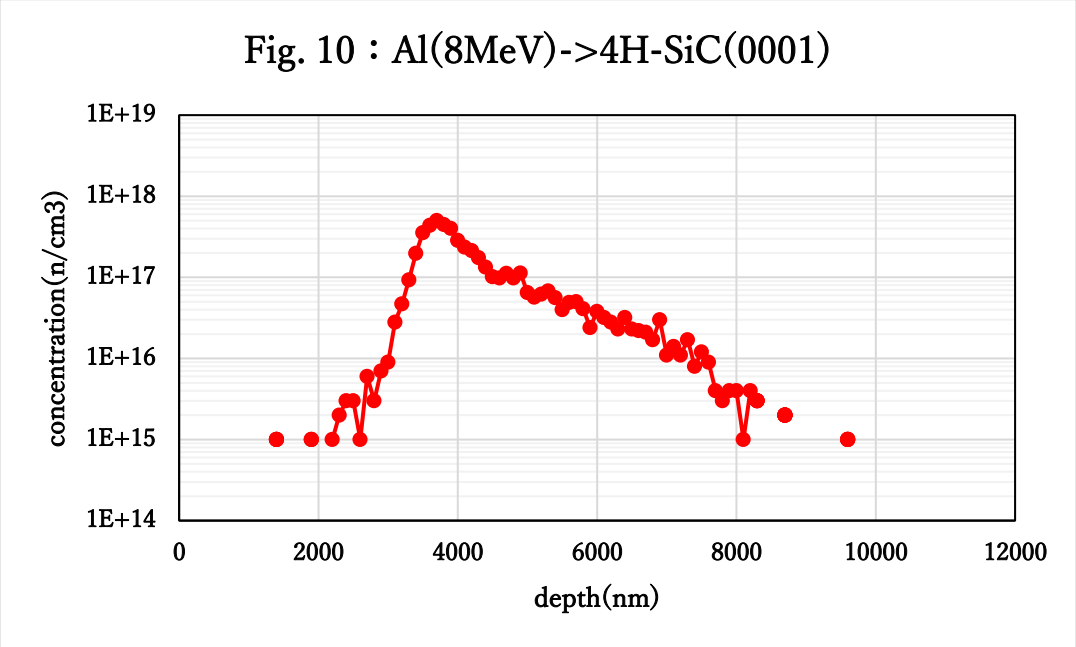

If the ion incident angle is tilted by 0.3 degrees or more from the graph of the critical channeling angle, the channeling phenomenon will be destroyed. In other words, high mechanical accuracy is required for the mechanism that installs the wafer. With conventional ion implanters, the accuracy of the wafer tilt is about ± 0.5 degrees. The latest ion implanters can be controlled with an accuracy of ± 0.1 degrees.

If channeling conditions are not used to achieve 8-micron penetration, a high energy implantation of around 30 MeV is required. In other words, a complicated and huge ion implanter such as a cyclotron is required. However, if channeling implantation is adopted, it can be handled by the ion implantation equipment used in the process.

In addition, the random implantation used in the normal ion implantation process increases the frequency of collisions with the target atom and increases the defects of the target atom. However, when ions invade along the channeling axis, the frequency of collisions with target atoms is suppressed, and defects due to ion implantation on the substrate are reduced. Therefore, it may be possible to realize a deep dopant distribution of several microns with few defects. Furthermore, since the ion implantation energy is kept low, there are merits such as being able to reduce the thickness of the mask. The research is underway on MOSFETs that utilize this technology to apply super-junction structures with deep dopant profiles in SiC power devices (8).

The current challenge is that the higher implantation doses will result in more defects due to incident ions and de-channeling. From the results reported so far, it is estimated that there is a critical dose at which the de-channeling begins. If the implanted dose is less than this critical dose, it is possible to obtain a profile in which incident ions penetrate deeply.

Figure 11 shows the analysis results of channeling implantation of 500 keV phosphorus into 4H-SiC. One can see that P ions have penetrated to about 1.5 microns.

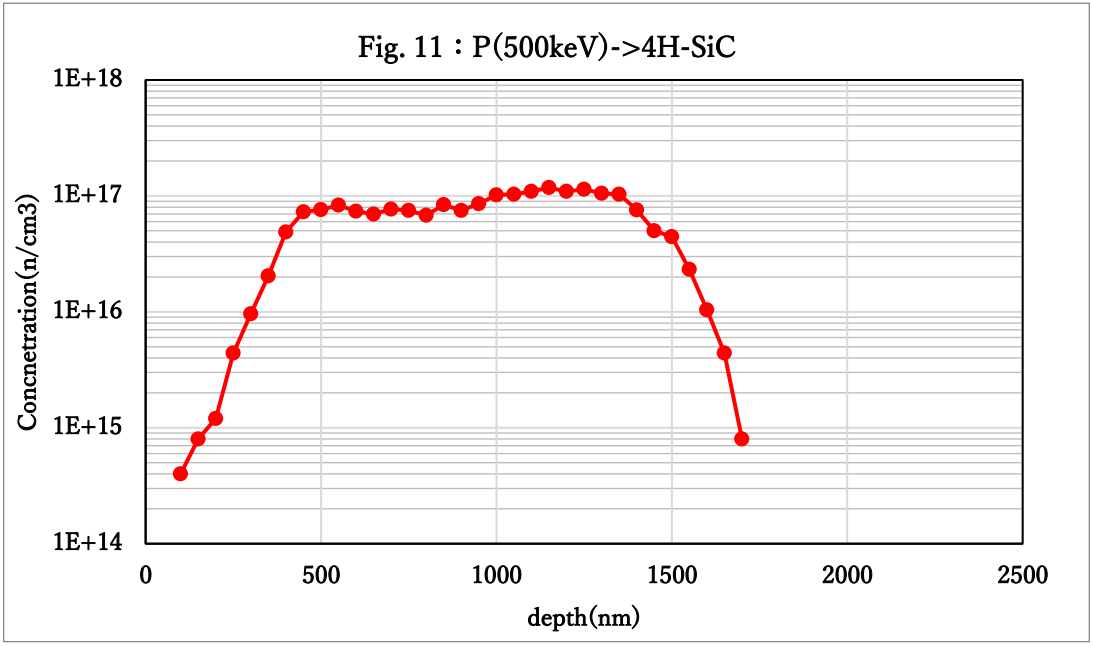

Figure 12 shows the simulation results of aluminum and nitrogen ion channeling implantation into 4H-SiC with the energy of 100 keV. The nitrogen profile shape is very different from that of aluminum. In addition, the penetration depth of incident ions is also shallow.

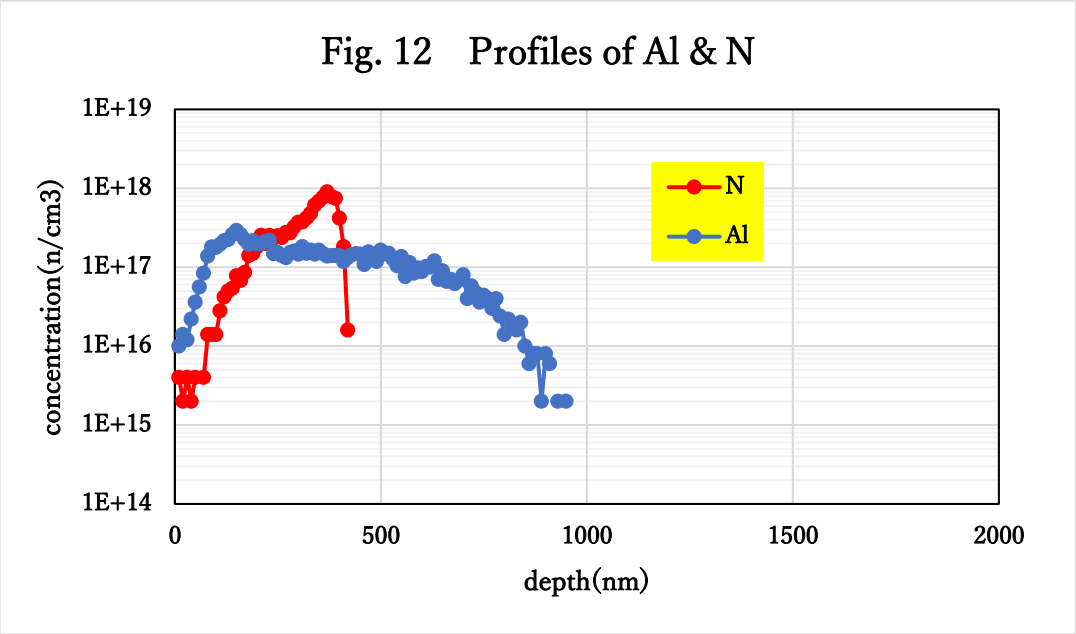

The reason for this is the effect of the difference in atomic radius between nitrogen ion and aluminum ion. Figure 13 shows the atomic number dependence of the atomic radius. The aluminum (Z = 13) and phosphorus (Z = 15) have the atomic

radius of 100 pm or more, but the nitrogen (Z = 7) has the atomic radius of about 60 pm. This difference in atomic radius is related to the implantation profile. In fact, we were able to reproduce the nitrogen ion implantation profile by changing the energy loss model considering this difference in atomic radius.

Fig. 13：atomic radius

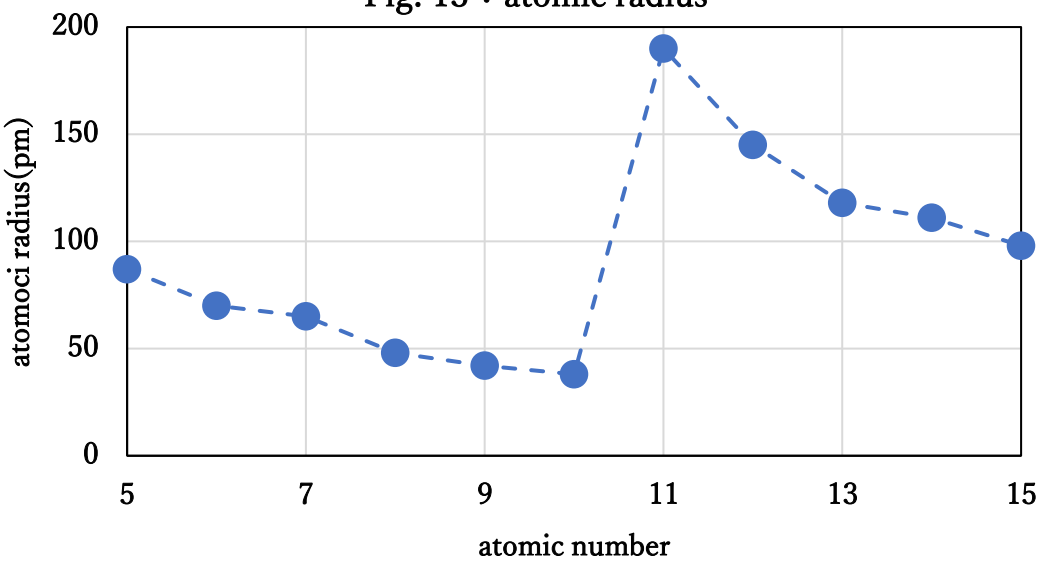

Figure 14 schematically shows the schematic view in which the atomic radius of the incident ion affects the collision phenomenon. When the atomic radius based on the arrangement of core electrons of the incident ion displayed in yellow becomes smaller, the interaction becomes weaker due to the relationship with the atomic radius of the target atom displayed in green, and the non-local electronic energy loss is essential instead of the local electronic energy loss. In other words, in the case of nitrogen, it is necessary to adopt a collision model different from that of aluminum and phosphorus.

Fig. 14：Collision with different atomic radius

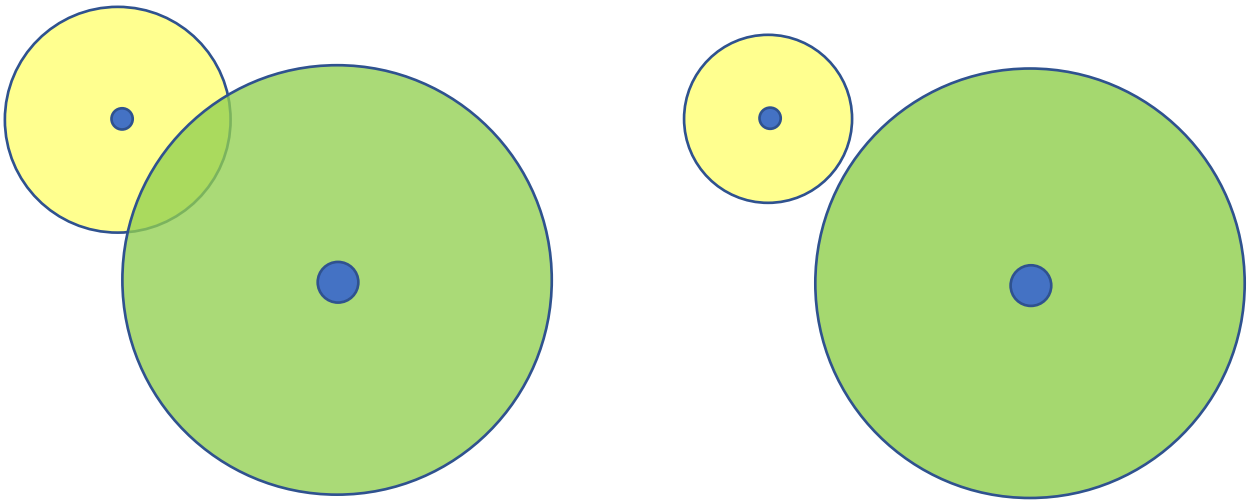

6. Effect of target temperature

In the case of SiC, it may be implanted at a high temperature to restore crystallinity. Figure 15 shows how the profile of incident ions changes when the target temperature increases. As the target temperature grows up, the lattice vibration amplitude increases, and de-channeling will begin. As a result, the profile shifts to the front side. Since the current simulation cannot consider the migration of atoms, a new analysis method is required to consider the defect recovery by high-temperature implantation.

Fig. 15：Al[100keV] into 4H-SiC(0001)

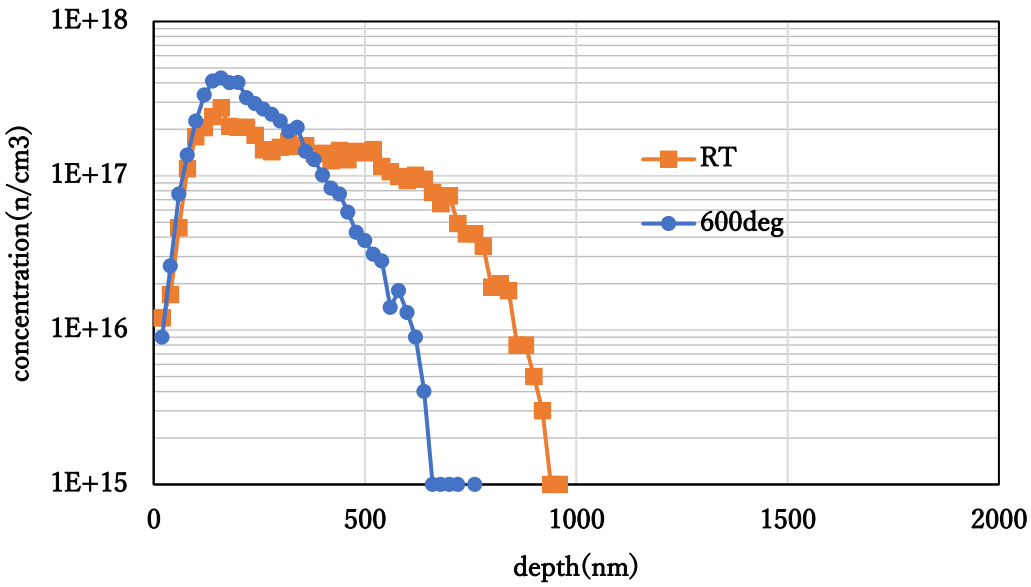

References

(1) R. Wada, et. Al, JJAP, 61, SC1033 (2022)
(2) M. Aoki, Oyo Buturi, November issue, P675 (2020)
(3) J. F. Ziegler, J. P. Biersack and U. Littmark, The stopping and ranges of ions in solids (1985)
(4) J. F. Ziegler, J. P. Biersack and U. Littmark, The stopping and ranges of ions in solids (1985)
(5) J. Lindhard, M. Scharff and H. E. Schiott: Dan. Vidensk. Seksk. Matt. Fys. Medd., V. 33, No.14, p. 1-42 (1963)
(6) M.T. Robinson, Proc. Of the Int. Conf. On Computer Simulations of Radiation effects in solids, 141 (1992)
(7) K. Nordlund, et.al, P.R.B, 94, 214109 (2016)
(8) PCT / US 2017/022240